Supplemental Information

Influence of oxygen and nitrate on Fe (hydr)oxide mineral transformation and soil microbial communities during redox cycling

Jacqueline Mejia,[1] Eric E. Roden,[2] and Matthew Ginder-Vogel[1]*

[1]The University of Wisconsin-Madison, Department of Civil and Environmental Engineering, Environmental Chemistry and Technology Program. 660 North Park St Madison, WI 53706

[2]The University of Wisconsin-Madison, Department of Geoscience. 1215 West Dayton Street Madison, WI 53706

*Corresponding Author

Matthew Ginder-Vogel

Address: 660 N Park Street. Madison, WI. 53706.

Email: mgindervogel@wisc.edu.

Phone: 608-262-0768

Fax: 608-262-0454

The Supporting Information contains 15 pages with a detailed description of sample preparation and analysis by X-ray Diffraction (XRD) and X-ray Absorption Spectroscopy (XAS). Additional Figures and Tables illustrate: the experimental summery (Table S1); nitrate concentrations during redox cycling with nitrate (Figure S1); aqueous Fe(II) concentrations, total Fe(II) concentrations and Fe (hydr)oxide mineralogy in Control Fe reducing reactors (Figure S2); taxa enriched by more than 1% in Control Fe reducing reactors (Figure S3); EXAFS spectra and fits for solid samples (Figures S4, S5 and S6); XRD patterns of solid samples (Figure S7 and S8); and characterization of 16S clone libraries (Table S2).

Solid Phase Analysis

X-ray Diffraction. XRD was utilized to verify the presence of crystalline Fe oxide phases used in the linear combination XAS analysis (described below). Samples for XRD analysis were ground into a fine powder using a mortar and pestle, packed into a boron silicate glass capillary tube, and sealed inside the glovebox to maintain anaerobic conditions. XRD patterns were collected using a Rigaku Rapid II X-ray diffractometer operating at 50 kV and 50 mA using Mo-Kα radiation. Diffraction data was collected over a 2.0 - 45° 2θ.

X-ray Absorption Spectroscopy. XAS data was collected either at GSE-CARS beamline 13-BMD at the Advanced Photon Source (APS) or beamline 4-1 at the Stanford Synchrotron Radiation Lightsource (SSRL). At the APS, energy selection was accomplished using a Si <111> double crystal monochromator and spectra were recorded in transmission using gas ionization chambers. At SSRL, energy selection was accomplished using a Si <220> double crystal monochromator, and fluorescent X-ray production was monitored using a Lytle detector with Söller slits and a 3 μx Mn filter to limit scattered incident X-rays. Samples for XAS analysis were ground into a fine powder and ~30 mg of the powder were diluted in boron nitride, packed into a sample holder (20 x 5 mm), and sealed with Kapton polyamide tape inside a glovebox to maintain anaerobic conditions during analysis. Between 2 and 5 extended X-ray absorption fine structure (EXAFS) spectra were collected and averaged for each sample. Averaged EXAFS spectra were then transformed from eV to $Å^{-1}$ to produce the function $\chi[k]$, where k ($Å^{-1}$) is the photoelectron wave vector, which was then weighted by k^3. Relative percentages of Fe mineral phases were determined by linear combination fitting of k^3-weighted EXAFS experimental spectra of Fe mineral standards using SIXPACK software.[1] The Fe mineral standards used were: two-line ferrihydrite ($Fe(OH)_3$), lepidocrocite (γ-FeOOH), goethite (α-FeOOH), maghemite (γ-

Fe_2O_3) and magnetite ($Fe^{II}Fe_2^{III}O_4$). In our results, maghemite represents partially oxidized magnetite.

Table S1. Experimental outline listing the days in which Fe reduction (addition of glucose) and Fe oxidation (addition of nitrate or dissolved oxygen) began.

Experiment	Initial Fe (hydr)oxide	Glucose addition (days)	Nitrate addition (days)	Oxygen addition (days)
Fe cycling with nitrate	**Lepidocrocite**	**0, 26, 55, 79**	**21, 49, 74, 101**	**-**
	Ferrihydrite	**0, 26, 55, 79**	**21, 49, 74, 101**	**-**
Fe cycling with molecular O_2	**Lepidocrocite**	**0, 26, 52, 77**	**-**	**21, 49, 74, 101**
	Ferrihydrite	**0, 26, 52, 77**	**-**	**21, 49, 74, 101**
Fe reduction	**Lepidocrocite**	**0**	**-**	**-**
	Ferrihydrite	**0**	**-**	**-**

Table S2. Characterization of 16S clone libraries.

Taxonomic Classification	Putative Physiology
Cupriavidus	Fe(II) phyllosilicate-oxidizing[2]
Ralstonia	Plant pathogen[3]
Geobacter	Fe(III)-reducing
Propionivibrio	Fermentative, acetate oxidation with ClO_4^-, ClO_3^-, NO_3^- or NO_2^{-4}
Desulfovibrio	Sulfate-reducing[5]
Sporomusa	Fermenting[6]
Dechloromonas	Fe(II)-oxidizing[7]
Desulfosporosinus	Sulfate-reducing; U(VI)-reducing[8]
Clostridium	Fermentative Fe(III)-reducing[9]
Desulfomicrobium	Sulfate-reducing[10]
Rhodocyclus	Denitrifying[11]
Sedimentibacter	Fermenting[12]
Acetobacterium	Acetate-producing[13]
Tolumonas	Toluene-producing[14]
Pseudomonas	Organic carbon degrading
Mycoplana	Decompose aromatic compounds[15]
Caulobacter	Organic carbon degrading[16]
Sulfurospirillum	Arsenate, Fe(III), Nitrate reducing[17]
Fusibacter	Fermenting[18]

Pleomorphomonas	Nitrogen-fixing[19]

Sulfate-reducing organisms in Fe redox cycling. Redox cycling with glucose and dissolved O_2 stimulates the enrichment of *Geobacter* (~28%) over other taxa (Figure 3). However, sulfate reducers (e.g. *Desulfovibrio* and *Desulfomicrobium*) and fermenting organisms (e.g. *Mycoplana and Propionivibrio*) are also detected at relatively low abundance levels (Figure 3). The increase in sulfate reducer abundance correlates with consumption of sulfate (0.5 mM initial concentration) during the first reducing period. Consistent with Fe(III) reduction occurring simultaneously with sulfate reduction and fermentation.[20,5,21]

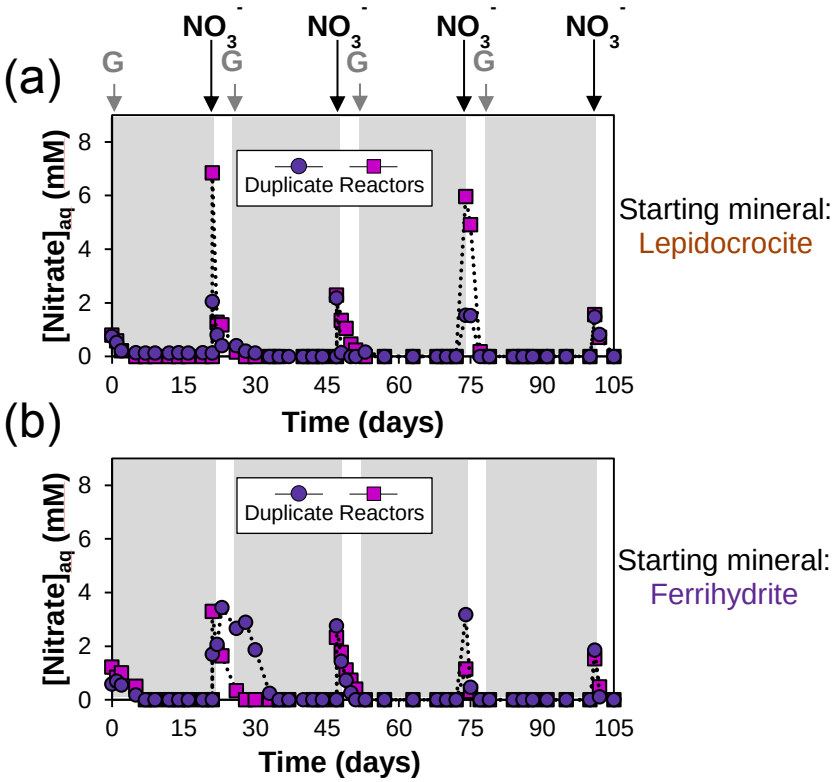

Figure S1. Impact of redox cycling with glucose (G) and nitrate (NO_3^-) on aqueous nitrate concentrations in reactors containing lepidocrocite (a) and ferrihydrite (b) as the starting minerals.

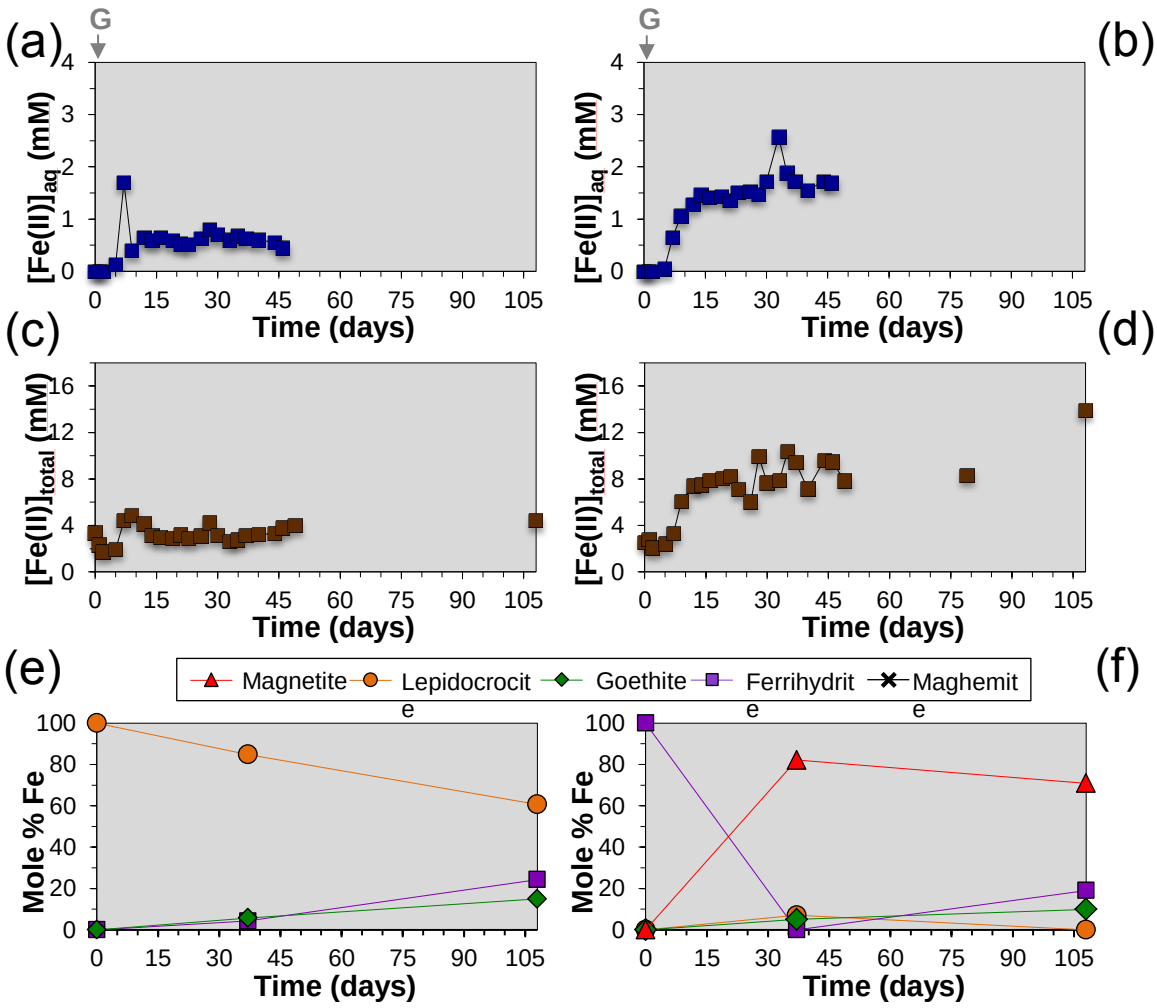

Figure S2. Impact of reduction with one glucose (G) addition on aqueous Fe(II) (a, b), total Fe(II) (c, d) and Fe (hydr)oxide mineralogy (e, f) in reactors containing lepidocrocite(a, c, e) or ferrihydrite(b, d, f) as the starting minerals.

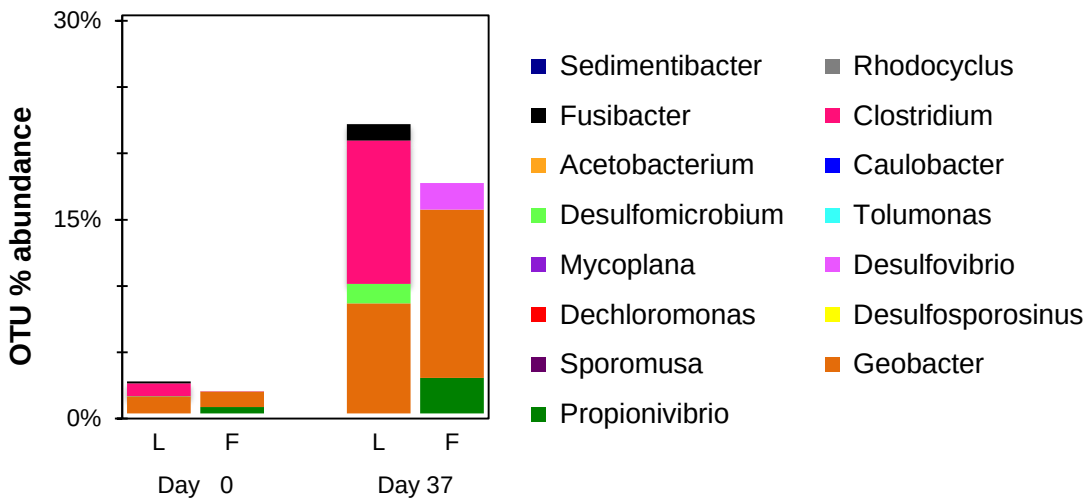

Figure S3. Taxa enriched by more than 1% (~25 reads) after 37 days of one reduction with glucose in the presence of lepidocrocite (L) and ferrihydrite (F) as the starting minerals. All taxa with functional classification are available in Table S1.

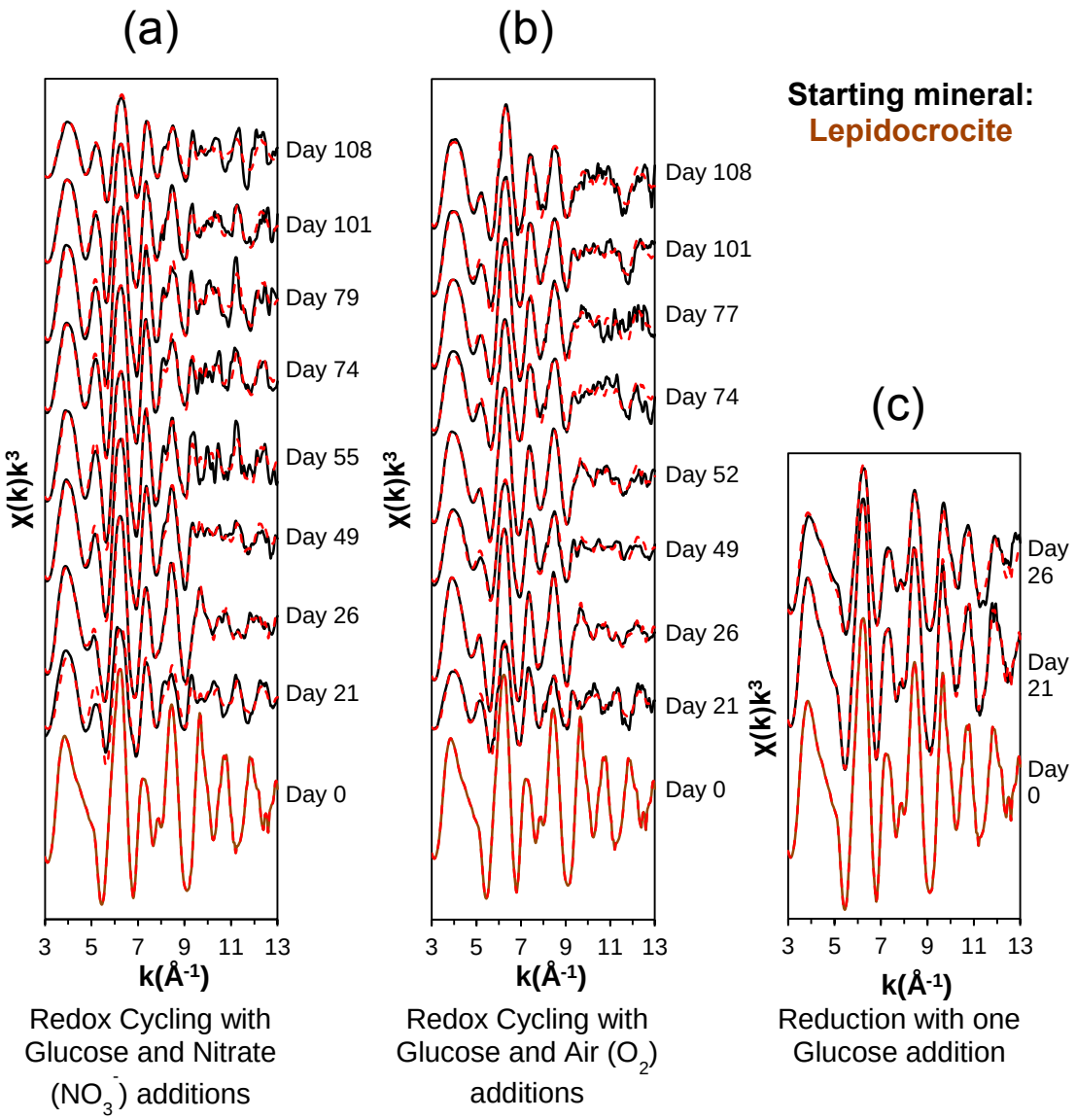

Figure S4. k^3-weighted EXAFS spectra (solid line) and linear combination fits (dotted line) for the solid phase products at the end of each reduction and oxidation periods. The starting mineral is lepidocrocite, and redox cycles are induced with glucose (G) and nitrate (NO_3^-) additions (a); glucose (G) and air (O_2) additions (b); and only one glucose addition (c).

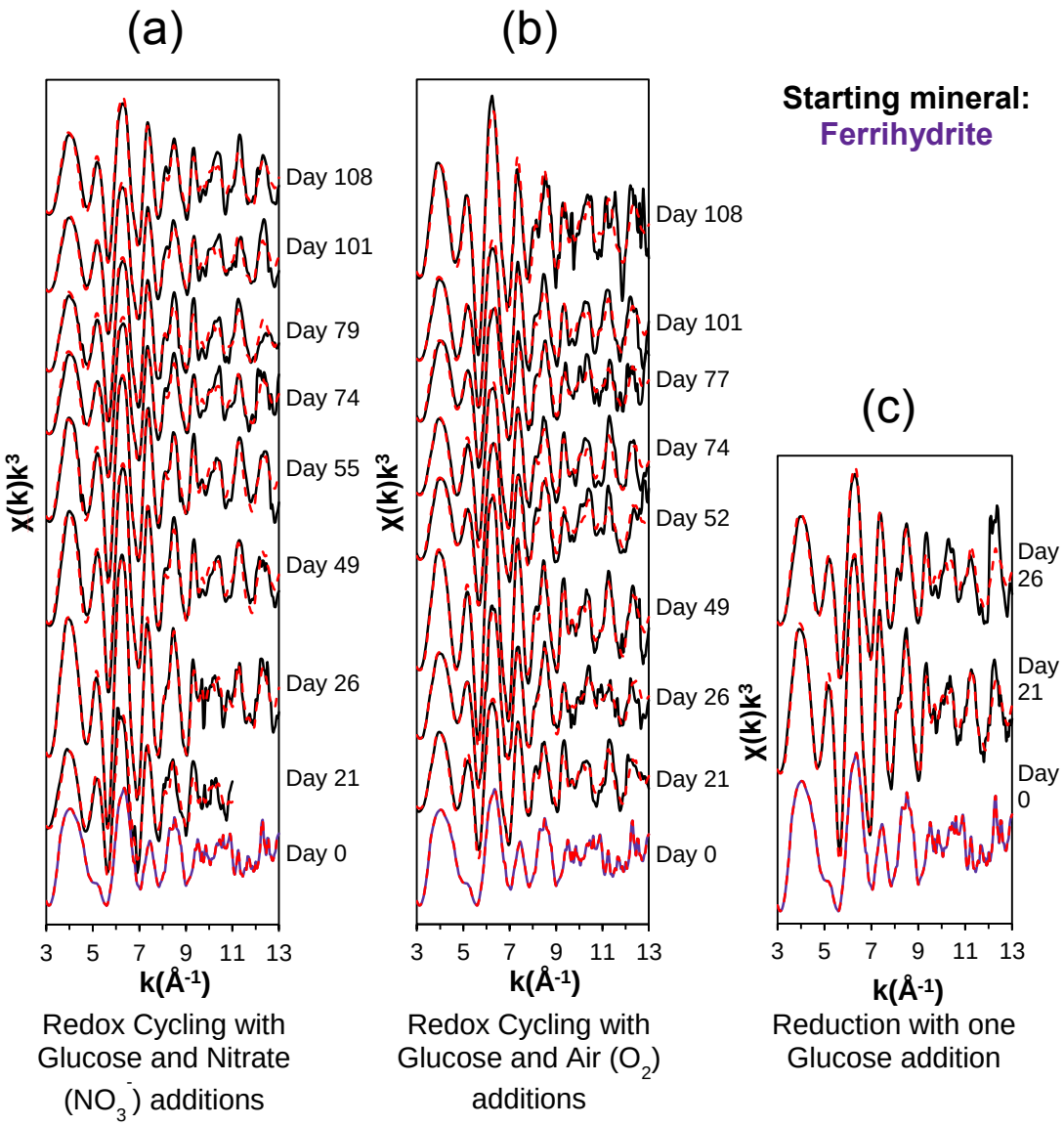

Figure S5. k^3-weighted EXAFS spectra (solid line) and linear combination fits (striped line) for the solid phase products at the end of each reduction and oxidation periods. The starting mineral is ferrihydrite, and redox cycles are induced with glucose (G) and nitrate (NO_3^-) additions (a); glucose (G) and air (O_2) additions (b); and only one glucose addition (c).

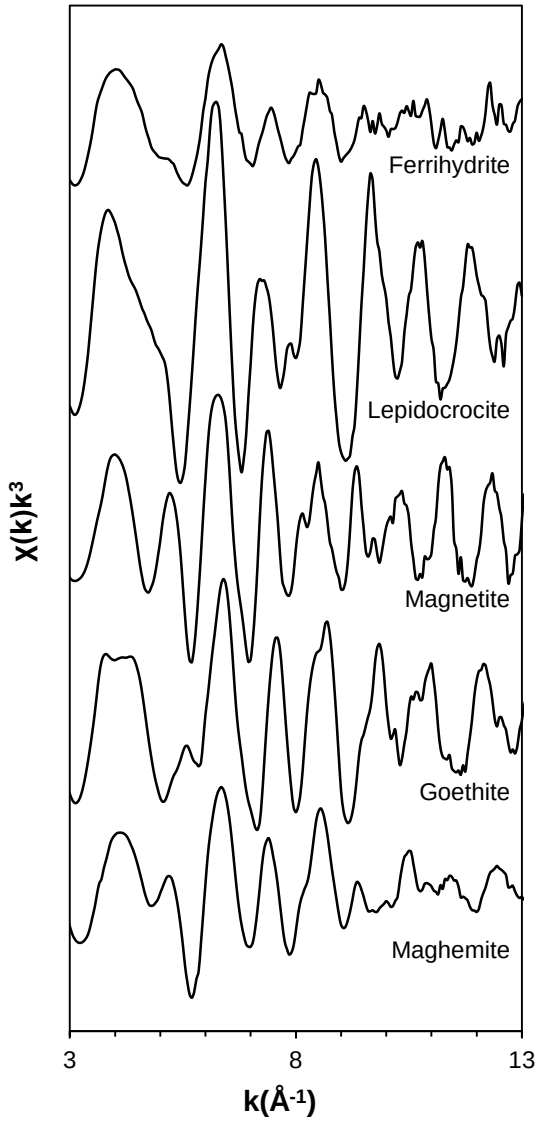

Figure S6. K^3-weighted EXAFS spectra (solid line) for the solid phase Fe mineral standards used in linear combination fitting.

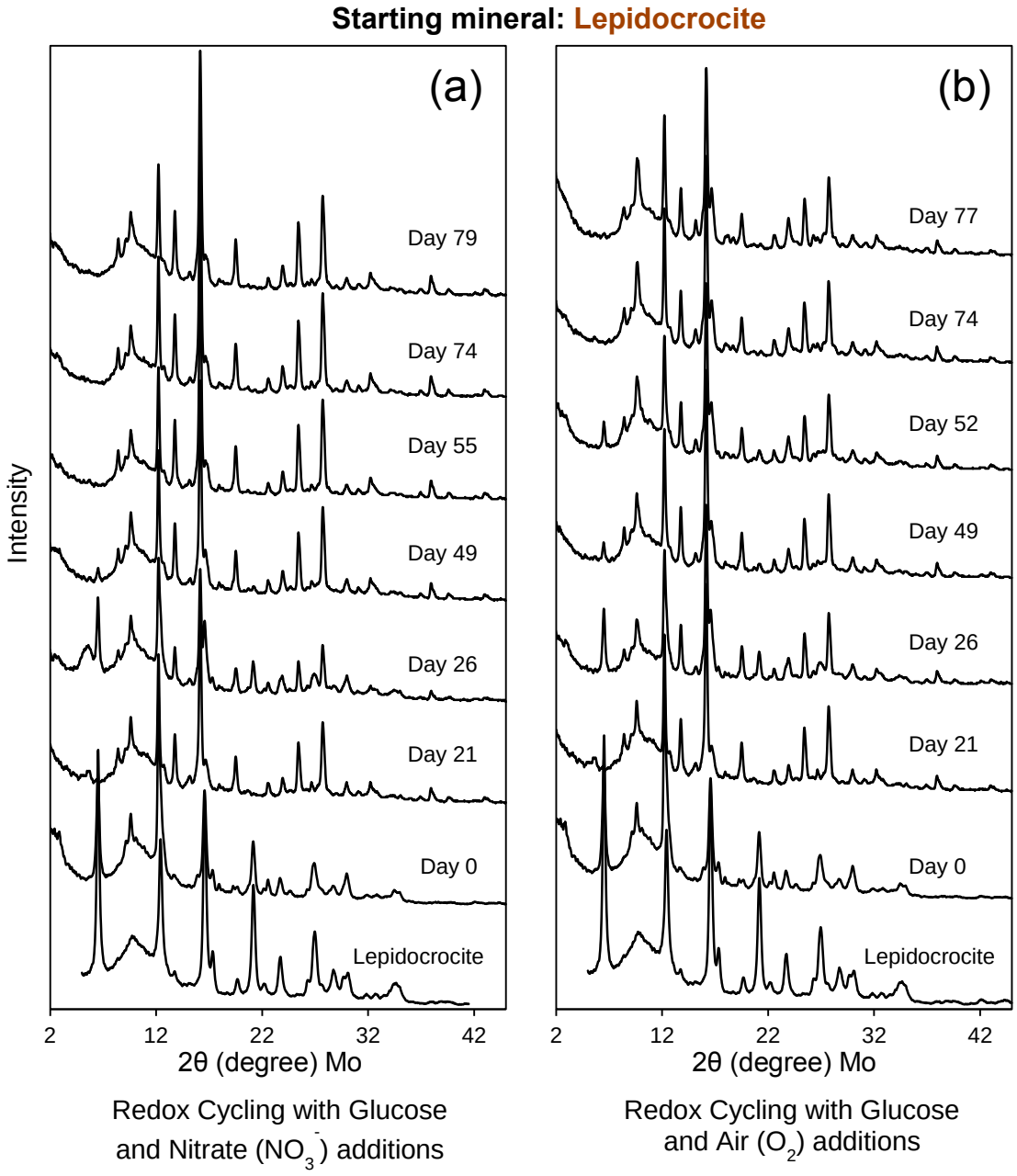

Figure S7. Powder X-ray diffraction spectra for the solid phase products at the end of each reduction and oxidation periods. The starting mineral is lepidocrocite, and redox cycles are induced with glucose (G) and nitrate (NO_3^-) additions (a) or glucose (G) and air (O_2) additions (b).

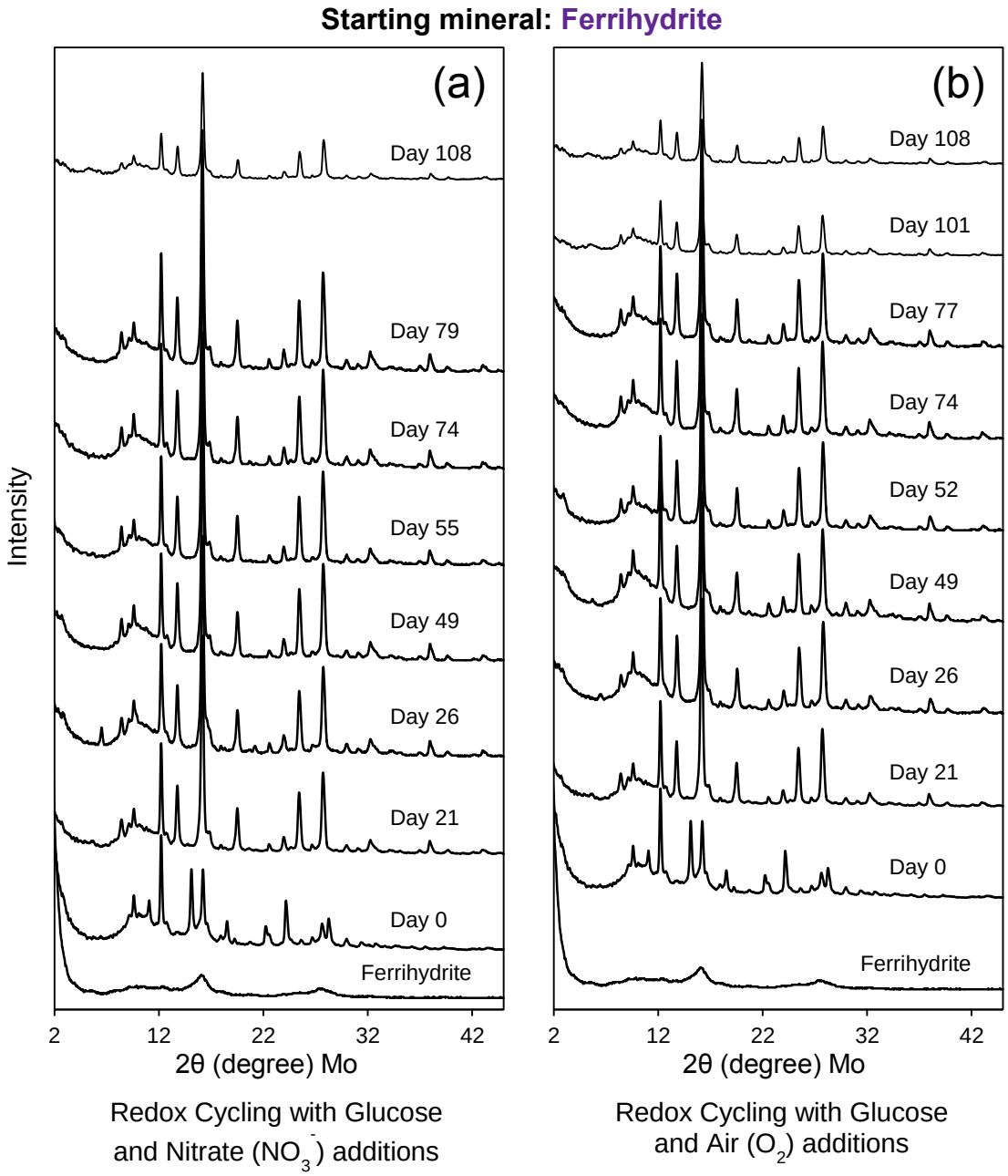

Figure S8. Powder X-ray diffraction spectra for the solid phase products at the end of each reduction and oxidation periods. The starting mineral is ferrihydrite, and redox cycles are

induced with glucose (G) and nitrate (NO_3^-) additions (a) or glucose (G) and air (O_2) additions (b).

References

(1) Webb, S. M. SIXpack: a graphical user interface for XAS analysis using IFEFFIT. *Phys. Scr.* **2005**, *2005* (T115), 1011.

(2) Benzine, J.; Shelobolina, E.; Xiong, M. Y.; Kennedy, D. W.; McKinley, J. P.; Lin, X.; Roden, E. E. Fe-phyllosilicate redox cycling organisms from a redox transition zone in Hanford 300 Area sediments. *Front. Microbiol.* **2013**, *4*, 388.

(3) Salanoubat, M.; Genin, S.; Artiguenave, F.; Gouzy, J.; Mangenot, S.; Arlat, M.; Billault, A.; Brottier, P.; Camus, J. C.; Cattolico, L.; et al. Genome sequence of the plant pathogen Ralstonia solanacearum. *Nature* **2002**, *415* (6871), 497–502.

(4) Thrash, J. C.; Pollock, J.; Torok, T.; Coates, J. D. Description of the novel perchlorate-reducing bacteria Dechlorobacter hydrogenophilus gen. nov., sp. nov. and Propionivibrio militaris, sp. nov. *Appl. Microbiol. Biotechnol.* **2010**, *86* (1), 335–343.

(5) Lentini, C. J.; Wankel, S. D.; Hansel, C. M. Enriched Iron(III)-Reducing Bacterial Communities are Shaped by Carbon Substrate and Iron Oxide Mineralogy. *Front. Microbiol.* **2012**, *3*.

(6) Dehning, I.; Stieb, M.; Schink, B. Sporomusa malonica sp. nov., a homoacetogenic bacterium growing by decarboxylation of malonate or succinate. *Arch. Microbiol.* **1989**, *151* (5), 421–426.

(7) Chakraborty, A.; Picardal, F. Induction of nitrate-dependent Fe(II) oxidation by Fe(II) in dechloromonas sp. Strain UWNR4 and Acidovorax sp. Strain 2AN. *Appl. Environ. Microbiol.* **2013**, *79* (2), 748–752.

(8) Cardenas, E.; Wu, W.-M.; Leigh, M. B.; Carley, J.; Carroll, S.; Gentry, T.; Luo, J.; Watson, D.; Gu, B.; Ginder-Vogel, M.; et al. Significant Association between Sulfate-Reducing Bacteria and Uranium-Reducing Microbial Communities as Revealed by a Combined Massively Parallel Sequencing-Indicator Species Approach. *Appl. Environ. Microbiol.* **2010**, *76* (20), 6778–6786.

(9) Scala, D. J.; Hacherl, E. L.; Cowan, R.; Young, L. Y.; Kosson, D. S. Characterization of Fe(III)-reducing enrichment cultures and isolation of Fe(III)-reducing bacteria from the Savannah River site, South Carolina. *Res. Microbiol.* **2006**, *157* (8), 772–783.

(10) Kushkevych, I. V. Growth of the Desulfomicrobium sp. strains, their sulfate- and lactate usage, production of sulfide and acetate by the strains isolated from the human large intestine. *Microbiol. Discov.* **2014**, *2* (1), 1.

(11) Smith, R. L.; Buckwalter, S. P.; Repert, D. A.; Miller, D. N. Small-scale, hydrogen-oxidizing-denitrifying bioreactor for treatment of nitrate-contaminated drinking water. *Water Res.* **2005**, *39* (10), 2014–2023.

(12) Breitenstein, A.; Wiegel, J.; Haertig, C.; Weiss, N.; Andreesen, J. R.; Lechner, U. Reclassification of Clostridium hydroxybenzoicum as Sedimentibacter hydroxybenzoicus gen. nov., comb. nov., and description of Sedimentibacter saalensis sp. nov. *Int. J. Syst. Evol. Microbiol.* **2002**, *52* (Pt 3), 801–807.

(13) Balch, W. E.; Schoberth, S.; Tanner, R. S.; Wolfe, R. S. Acetobacterium, a New Genus of Hydrogen-Oxidizing, Carbon Dioxide-Reducing, Anaerobic Bacteria. *Int. J. Syst. Bacteriol.* **1977**, *27* (4), 355–361.

(14) Fischer-Romero, C.; Tindall, B. J.; Juttner, F. Tolumonas auensis gen. nov., sp. nov., a Toluene-Producing Bacterium from anoxic sediments of a freshwater lake. *Int. J. Syst. Bacteriol.* **1996**, *46* (1), 183–188.

(15) Urakami, T.; Oyanagi, H.; Araki, H.; Suzuki, K.-I.; Komagata, K. Recharacterization and Emended Description of the Genus Mycoplana and Description of Two New Species, Mycoplana ramosa and Mycoplana segnis. *Int. J. Syst. Bacteriol.* **1990**, *40* (4), 434–442.
(16) Abraham, W.-R.; Strompl, C.; Meyer, H.; Lindholst, S.; Moore, E. R. B.; Christ, R.; Vancanneyt, M.; Tindall, B. J.; Bennasar, A.; Smit, J.; et al. Phylogeny and polyphasic taxonomy of Caulobacter species. Proposal of Maricaulis gen. nov. with Maricaulis maris (Poindexter) comb. nov. as the type species, and emended description of the genera Brevundimonas and Caulobacter. *Int. J. Syst. Bacteriol.* **1999**, *49* (3), 1053–1073.
(17) Stolz, J. F.; Ellis, D. J.; Blum, J. S.; Ahmann, D.; Lovley, D. R.; Oremland, R. S. Note: Sulfurospirillum barnesii sp. nov. and Sulfurospirillum arsenophilum sp. nov., new members of the Sulfurospirillum clade of the -Proteobacteria. *Int J Syst Bacteriol* **1999**, *49* (3), 1177–1180.
(18) Ravot, G.; Magot, M.; Fardeau, M.-L.; Patel, B. K. C.; Thomas, P.; Garcia, J.-L.; Ollivier, B. Fusibacter paucivorans gen. nov., sp. nov., an anaerobic, thiosulfate-reducing bacterium from an oil-producing well. *Int. J. Syst. Bacteriol.* **1999**, *49* (3), 1141–1147.
(19) Xie, C.-H. Pleomorphomonas oryzae gen. nov., sp. nov., a nitrogen-fixing bacterium isolated from paddy soil of Oryza sativa. *Int. J. Syst. Evol. Microbiol.* **2005**, *55* (3), 1233–1237.
(20) Stucki, J. W.; Lee, K.; Goodman, B. A.; Kostka, J. E. Effects of in situ biostimulation on iron mineral speciation in a sub-surface soil. *Geochim. Cosmochim. Acta* **2007**, *71* (4), 835–843.
(21) Melton, E. D.; Swanner, E. D.; Behrens, S.; Schmidt, C.; Kappler, A. The interplay of microbially mediated and abiotic reactions in the biogeochemical Fe cycle. *Nat. Rev. Microbiol.* **2014**, *12* (12), 797–808.